



**INSTYTUT BADAŃ SYSTEMOWYCH
POLSKIEJ AKADEMII NAUK**

TECHNIKI INFORMACYJNE TEORIA I ZASTOSOWANIA

Wybrane problemy
Tom 4 (16)

poprzednio

**ANALIZA SYSTEMOWA W FINANSACH
I ZARZĄDZANIU**

Pod redakcją
Andrzeja MYŚLIŃSKIEGO

Warszawa 2014



**INSTYTUT BADAŃ SYSTEMOWYCH
POLSKIEJ AKADEMII NAUK**

TECHNIKI INFORMACYJNE TEORIA I ZASTOSOWANIA

Wybrane problemy
Tom 4 (16)

poprzednio

**ANALIZA SYSTEMOWA W FINANSACH
I ZARZĄDZANIU**

Pod redakcją
Andrzeja Myślińskiego

Warszawa 2014

Wykaz opiniodawców artykułów zamieszczonych
w niniejszym tomie:

Prof. Bernard De BAETS

Dr hab. Ewa BEDNARCZUK, prof. PAN

Dr hab. inż. Wiesław KRAJEWSKI, prof. PAN

Dr hab. inż. Andrzej MYŚLIŃSKI, prof. PAN

Dr inż. Jan W. OWSIŃSKI

Dr hab. Dominik ŚLĘZAK, prof. UW

Prof. dr hab. inż. Andrzej STRASZAK

Prof. dr hab. inż. Stanisław WALUKIEWICZ

Copyright © by Instytut Badań Systemowych PAN
Warszawa 2014

ISBN 83-894-7555-3

VASCULAR PATTERN IDENTIFICATION BY LINE TRACKING METHOD

Piotr Fronc

*Systems Research Institute, Polish Academy of Sciences,
Ph. D. Studies, Warsaw, Poland,
fronc.piotr@gmail.com*

Abstract. The paper deals with biometric identification based on vascular patterns matching. The image of a finger has been acquired using LED infrared light combined with a visible light filter. To improve the quality of image it has been smoothed. The vascular pattern has been extracted using line tracking approach. Statistical approach has been used to verify matching the obtained and given pattern images. Experimental results are provided and discussed.

Key words: vascular biometrics, biometric authentication, image acquisition

1 INTRODUCTION

In recent years biometric identity verification gained much attention [1, 3]. Apart from methods like fingerprint identification, known for centuries, new means of identification have been developed. These include, among others, iris pattern recognition [1], automated face recognition and vein pattern recognition [4]. Behavioral methods, which include handwriting dynamics as well as walking dynamics were also established [1].

Biometric systems can be classified into two main groups: biometric verification and identification systems. Methods discussed in this paper can be utilised in both groups, however, we will focus on verification systems only. A biometric verification system is such that aims at confirming the identity of an individual [1]. Applications of personal verification systems vary from access control to financial operations authorization. On the other hand, a biometric identification system is determined as a system, the purpose of which is to identify an individual among population. Such systems are often applied in the field of forensics. Vascular biometrics puts its interest into vein pattern underneath human skin. Patterns that are regarded as unique among the population can be obtained from fingers, palms and faces. A biometric system has two modes of operation. These are: enrollment and template matching.

This paper focuses on methods of image preprocessing and pattern segmentation of finger vein patterns. Biometric templates are obtained from

subjects, connected to personal data and stored in enrollment mode. Sections 2 and 3 cover techniques related with the enrollment process. In template matching mode, a template is obtained from individual in question and matched against data stored during enrollment process. Section 4 describes simple matching algorithm and a brief evaluation of matching is given. Vein pattern extraction algorithm described by Miura et al. [2] has been selected as a reference method. Algorithm and preconditions were modified in order to meet restrictions resulting - among others - from image acquisition device construction, namely:

- image preprocessing - image smoothening and normalization were implemented;
- during image segmentation - simple cycle detection has been implemented;
- during image segmentation - spatial reduction and tresholding has been modified;
- during image segmentation - only one locus space is created in order to decrease memory footprint; Locus space is updated by subsequent algorithm iterations;
- region of interest segmentation - due to different device construction, image is statically cropped.

2 VASCULAR PATTERN IMAGE ACQUISITION

Vascular biometric systems operate on patterns of veins underneath human skin. There are several widely used regions of human body from which vein patterns can be obtained. These are hand palms, fingers and face. Vein patterns from these regions are recognized as unique, similarly to finger print patterns. In terms of unauthorized pattern usage, however, measured by ability to obtain vein pattern without subject's knowledge and permission, finger vein and palm vein patterns seem to represent a vast improvement to system's security over finger printing methods [4].

Vein pattern is obtained by capturing image form CCD sensor. Acquisition subject is first illuminated with infra-red or near infra-red light. Oxidated hemoglobin within subject's veins absorbs infra red radiation, thus veins in the image will appear as dark lines [7, 8]. Vein patterns of different fingers of the same person are not correlated, which meas that every vein pattern of each finger can be treated as a template of distinct origin.

2.1 Apparatus

A custom vein image acquisition device has been constructed and in details is discussed in [10]. Below, most important features are given. Device consists of four main elements: CCD camera, two LED matrices, IR filter and framegrabber. Finger is illuminated by near infrared light emitted by LED matrices. IR filter lies below LED matrices. CCD sensor lies below an IR filter and is connected to a framegrabber. Through frame grabber, image is transferred to the PC. Ideogram and actual device image are presented in Fig. 1a and 1b, respectively.

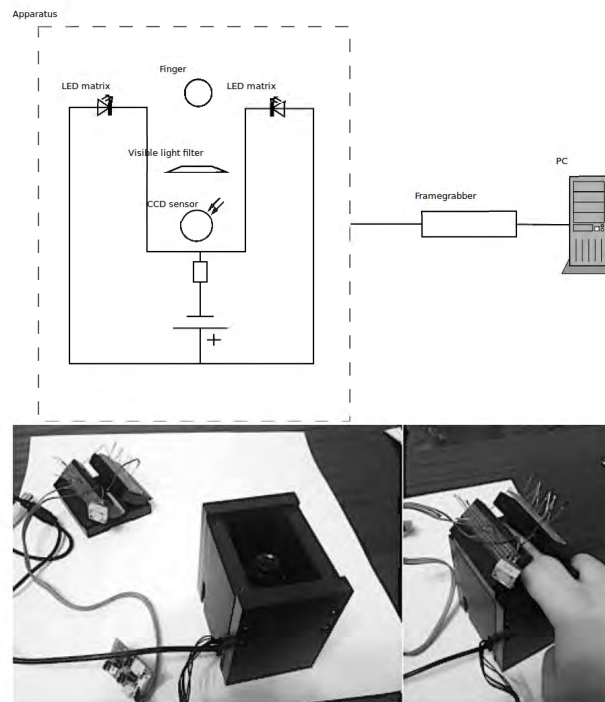


Fig. 1. 1a. Device ideogram; 1b. Device prototype.

Lighting subsystem consists of two LED matrices. Each matrix consists of 5 LEDs organized in a row. Each LED emits near-infrared light of wave length $880nm$. Wave length $880nm$ was chosen experimentally basing on absorption curves given in [7, 8]. For discussed wave length oxidated hemoglobin light absorption is near its local maximum for infra-red

range while unoxidated hemoglobin light absorption is relatively low. Also, CCD sensor light absorption is still relatively high (above 40%).

2.2 Image pre-processing

After the acquisition the image is pre-processed, since the contrast level of the image is low. The pre-processing method used by the author comprises of image multiplication and normalization. In the first step the acquired image is multiplied by itself, i.e.,

$$F'(x, y) = F(x, y) * F(x, y), \quad (1)$$

where $F(x, y)$ denotes a value of the image function F in a pixel characterized by the point coordinates $x, y \in \mathbb{N} \times \mathbb{N}$. Function $F'(x, y)$ denotes the result of the functions multiplication. This operation allows to obtain better contrast of veins, as they appear as darker regions of the image. Thus multiplication results in distinctively lower pixel values than the background. The multiplied image is then normalized in the following way:

$$F_n(x, y) = \frac{F'(x, y)}{F_{max}}, \quad (2)$$

where F_{max} is defined as

$$F_{max} = \max_{(x,y) \in \Omega} F'(x, y), \quad (3)$$

where $\Omega \subset \mathbb{N} \times \mathbb{N}$ is two dimensional domain occupied by the image.

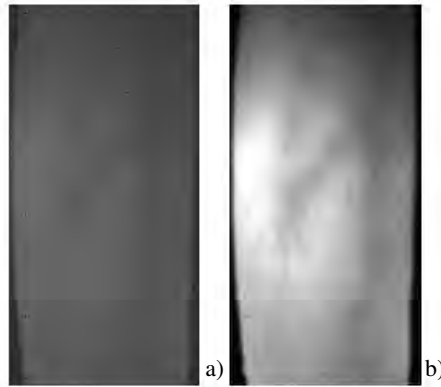


Fig. 2. Obtained finger vein image. a) original image, b) pre-processed image

After normalization process is finished, pixel values of the normalized image are from the range $< 0, 1 >$. Because image is then interpreted as a grayscale bitmap image, each pixel is then multiplied by value 255. Images before and after pre-processing process are presented in Fig. 2a and 2b, respectively. In Fig. 3a and 3b, cross-section profile of a vein before and after pre-processing are given, respectively. It can be observed, that the vein cross section after preprocessing is shaped more valley-like. Maximum and minimum pixel values are more distant from each other which improves the segmentations process described in the following sections.

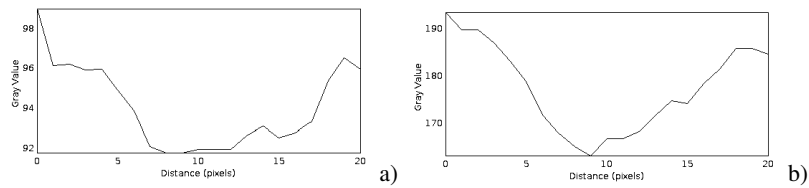


Fig. 3. Cross section profile of a vein taken from raw (a) and pre-processed (b) images

2.3 Region of Interest (ROI) selection

Region of interest selection is an important aspect of preparation towards feature extraction. Many papers deal with this problem and many approaches are used [5, 6]. In this paper, region of interest selection is based on acquisition device construction points and is done statically by cropping the image acquired. Thus, the method described in this paper is susceptible to excessive finger displacement within the acquisition device. Comparable to other methods described in literature, excessive finger rotation should also affect further recognition process as image of veins substantially changes for spacial dependencies and light dispersion in human tissue reasons.

3 FEATURE EXTRACTION

3.1 Overview

Enrollment process, is presented in Fig. 4. Below, a short description is given:

1. Process starts with vein image acquisition;

2. Image is normalized;
3. Vein pattern is extracted;
4. Template is stored to database.

System user initiates the enrollment action and puts his or her finger on the device for scanning. Obtained pattern is transformed into template and categorized with subject's unique identification number and finger ID. After template creation, it is stored into database.

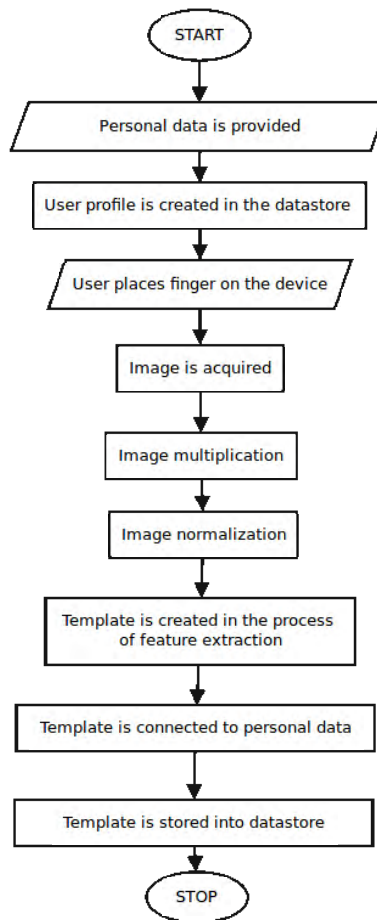


Fig. 4. Enrollment block diagram.

3.2 Line tracking algorithm

Repeated line tracking algorithm (as presented by Miura et al. [2]) was chosen for implementation as a reference method. The following symbols and variables are used in the algorithm description:

- R_f - image subspace inside the finger outline;
- $F(x_i, y_i)$ - value of the i -th pixel;
- (x_s, y_s) - starting point coordinates; $(x_s, y_s) \in R_f$;
- (x_c, y_c) - current tracking point coordinates; $(x_c, y_c) \in R_f$;
- D_h - parameter to indicate horizontal movement direction:

$$D_h = \begin{cases} (1, 0) & \text{if } r_2 < 1 \\ (-1, 0) & \text{if } r_2 \geq 1; \end{cases} \quad (4)$$

- D_v - parameter to indicate vertical movement direction:

$$D_v = \begin{cases} (0, 1) & \text{if } r_2 < 1 \\ (0, -1) & \text{if } r_2 \geq 1; \end{cases} \quad (5)$$

where r_n is a random number, drawn uniform distribution: $0 \leq r_n \leq n, n \in \mathbb{N}$. Let T_c be a space containing all previous tracking points (after [2] — locus table); N_c is a space of potential achievable tracking points defined as:

$$N_c = T'_c \cap R_f \cap N_r(x_c, y_c). \quad (6)$$

Set $N_r(x_c, y_c)$ consists of neighbor points of current tracking point (x_c, y_c) defined as [2]:

$$N_r(x_c, y_c) = \begin{cases} N_3(D_h)(x_c, y_c) & \text{if } r_{100} < p_h, \\ N_3(D_v)(x_c, y_c) & \text{if } p_h + 1 \leq r_{100} < p_h + p_v, \\ N_8(x_c, y_c) & \text{if } p_h + p_v + 1 \leq r_{100}, \end{cases} \quad (7)$$

where:

- N_3 is a set of three neighbor points;
- N_8 is a set of eight neighbor points of the current tracking point;
- p_h is a parameter reflecting probability of electing three neighbor points in horizontal direction ($p_h \in \langle 0, 100 \rangle$ in the discussed implementation $p_v = 10$);
- p_v is a parameter reflecting probability of electing three neighbor points in vertical direction ($p_v \in \langle 0, 100 \rangle$, in the discussed implementation $p_v = 90$);

– V_l is a parameter evaluating the next possible current tracking point

$$V_l = \max_{(x'_c, y'_c) \in N_c} \left\{ F(x_c + r \cos \theta'_c - \frac{W}{2} \sin \theta'_c, y_c + r \sin \theta'_c + \frac{W}{2} \cos \theta'_c) \right. \\ \left. + F(x_c + r \cos \theta'_c + \frac{W}{2} \sin \theta'_c, y_c + r \sin \theta'_c - \frac{W}{2} \cos \theta'_c) \right. \\ \left. - 2F(x_c + r \cos \theta'_c, y_c + r \sin \theta'_c) \right\},$$

where W is width of the vein's color-depth profile (in the discussed implementation $W = 10$), r is a radius of the aforementioned profile, θ'_c is an angle between line parallel to x axis passing through the current tracking point (x_c, y_c) and line segment originating in the current tracking point and ending in the potential tracking point (x'_c, y'_c) . Graphical representation of the above mentioned variables is given in Fig.5.

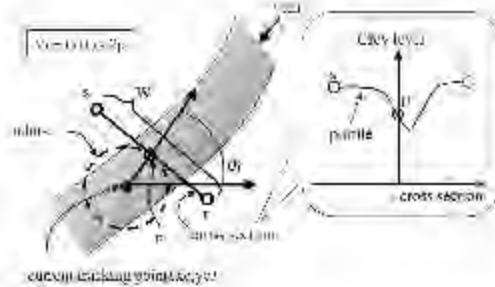


Fig. 5. Dark line detection [2]

Below, the algorithm is given. T_r denotes cumulative locus space for repetitive line trackings.

Step 1. Determine starting point of the algorithm. Starting point $(x_s, y_s) \in R_f$ is chosen randomly with uniform distribution. The starting point is now the current tracking point (x_c, y_c) .

Step 2. Detect tracked line direction and move current tracking point: T_c is initialized. N_c is calculated. Then, direction of the tracked line is detected by repetitive calculation of the V_l value for pixels which are in N_c set. A new current tracking point (x'_c, y'_c) is chosen for the maximal

value of V_l and a previous tracking point is stored into T_c . Repeat until V_l is negative.

Step 3. Update cumulative locus space: T_r is updated with elements of T_c .

Step 4. Repeat steps 1—3 Steps 1—3 are repeated for a previously established number of times n_{rep} .

Step 5. Spatial reduction of the template obtained and storage. The resulting locus space T_r is binarized using threshold value (in this implementation, threshold value has been set to 80) and read in non-overlapping blocks of size $n_{red} \times n_{red}$. The n_{red} parameter is chosen experimentally depending on input image resolution (as mentioned above, in this implementation, spatial reduction is not performed, so $n_{red} = 1$). The reduced locus space T'_r is created by storing the average values from each block. T'_r is then rebinarized using multiple threshold to create three classes of points: background, ambiguous region and veins [2]. In this implementation, however, a single threshold is implemented with value set to 80. Template T'_r is stored into template database.

4 RESULTS

4.1 Overview

Below, in Fig. 6, the full cycle of template preparation is presented.

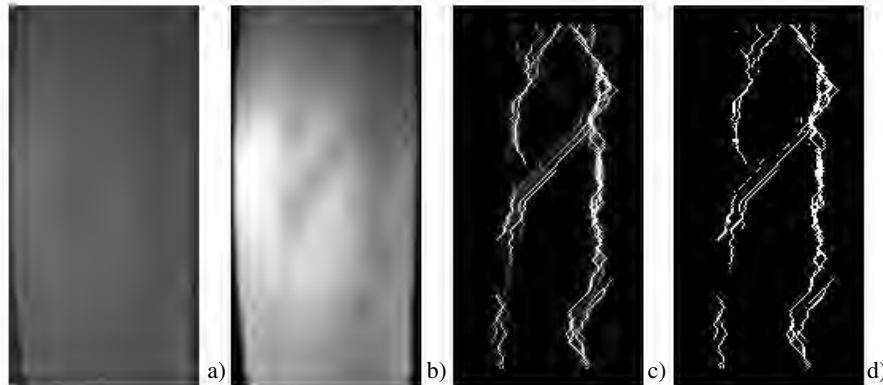


Fig. 6. Full template extraction cycle: (a) raw image, (b) pre-processed image, (c) line tracking product, (d) final binarized template

The following alterations were made to the algorithm proposed in the preceding section: the obtained intermediate form of the template is not

spacially reduced. The spacial reduction was performed in [2] in order to decrease matching time. In this paper, the author did not focus on this aspect, rather exploring the segmentation process alone. Also, the obtained intermediate image is thresholded into two groups of pixels: veins and background, leaving the uncertain region unallocated.

4.2 Evaluation of feature extraction accuracy

In [2], a method was proposed of template matching. In this paper, however, a more generic method of evaluation of feature extraction algorithm, described in [9] was used. Evaluation is done by extracting features consecutively from the same image and calculating a Matched Pixel Ratio (*MPR*):

$$MPR = \frac{2 \sum_{x,y} I(x,y)T(x,y)}{\sum_{x,y} I(x,y) + \sum_{x,y} T(x,y)}, \quad (8)$$

where I is the input image and T is the previously obtained template.

This method was used to evaluate the accuracy of feature extraction itself. Since the algorithm includes randomized operations, the output differs each execution. The *MPR* coefficient reflects the 'likeness' of two products of the algorithm. Higher *MPR* values represent a better match.

The following experiment has been conducted in order to establish algorithm parametrization: for $500 \leq n_{rep} \leq 5000$ one thousand matching processes were performed. Mean *MPR* value was calculated for each of the classes (division to classes by n_{rep} value). In Fig. 7 $MPR(n_{rep}) = N_n$ function is presented.

It can be observed, that n_{rep} value above 1500 does not result in significantly higher *MPR* values. This suggests that, since high number of repetitions is the key factor to the algorithm's execution time, using n_{rep} value of 2000 is sufficient in terms of satisfying *MPR* values. However, as can be seen in Fig. 8, for number of repetitions below 4500, veins are not fully extracted.

In Fig. 9 n_{rep} to execution time dependency is presented. Since this dependency is of linear nature, increasing the n_{rep} parameter value does not result in excessive computation cost. What is more, each iteration of the algorithm is independent in terms of results of subsequent algorithm runs. Overall execution time can be shortened by parallelizing algorithm's iterations.

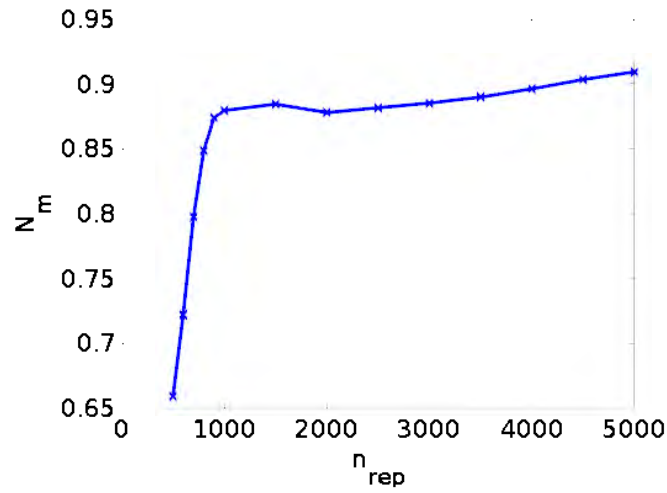


Fig. 7. $MPR(n_{rep})$ Values of MPR function depending on the number of repetitions n_{rep}

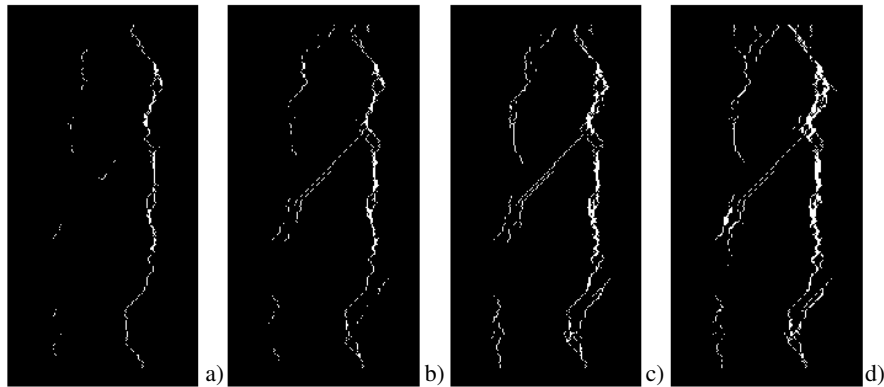


Fig. 8. Extracted pattern after thresholding with n_{rep} : a) 1500, b) 2500, c) 3500, d) 4500

4.3 Vein pattern displacement and rotation

The described matching method is susceptible to image rotation and offset. This is due to the nature of the method which essentially focuses on comparing the values of corresponding pixels in input and template images. Introducing a region of interest segmentation stage, following pre-processing stage, should improve the results. In Fig. 10a an artificial vein image is presented. In Fig 10b, a rotated version of the image is presented

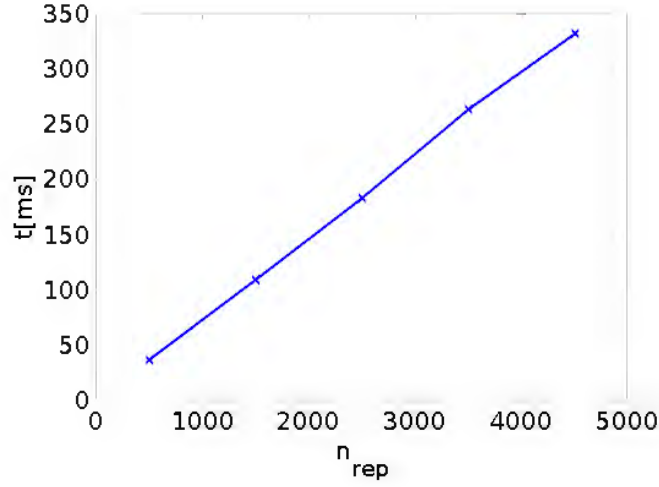


Fig. 9. n_{rep} to execution time dependency

(3°). In Fig. 10c, the vein image was shifted. Matching results for these images are given in Table 1.

input	template	MPR
artificial(original)	artificial(original)	0.91
artificial(original)	artificial(rotated)	0.25
artificial(original)	artificial(offset)	0.17

Table 1. MPR values for artificial vein image rotation and displacement

4.4 Light conditions

In order to evaluate extraction algorithm's susceptibility to lightning conditions, artificial vein image used in previous section was altered by decreasing image brightness and adding non-uniform lightning conditions. In Fig 11a, an original image is presented. In Fig 11b, altered image is presented. In figures 11c and 11d, products of feature extraction for both input images are presented respectively. The average MPR value computed for these images ($n_{rep} = 4500, 1000$ algorithm runs) is 0.48. This MPR value decrease is due to vein pattern deformation caused by both darker and lighter parts of the altered image. This leads to the conclusion,

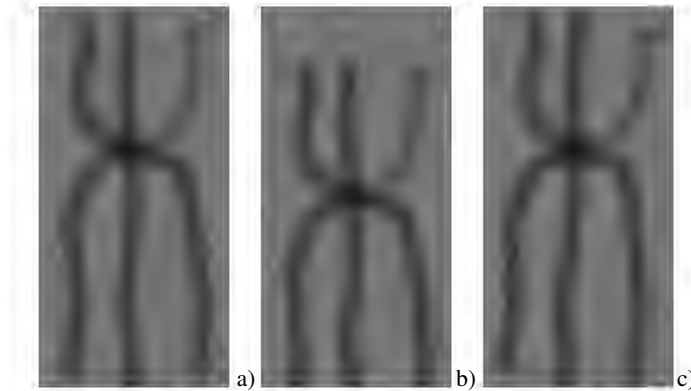


Fig. 10. Artificial vein image: a) original image, b) rotated image, c) displaced image

that the overall process consisting of feature extraction and matching is more prone to both image displacement and rotation, than lightning conditions. However, providing equally distributed illumination seems to be a necessary condition in order to secure a proper vein pattern extraction. Proposed image pre-processing method is not suitable for provided image, as it loses image information by both transforming "shadow" and "overburnt" regions into indistinctive dark and light areas respectively.

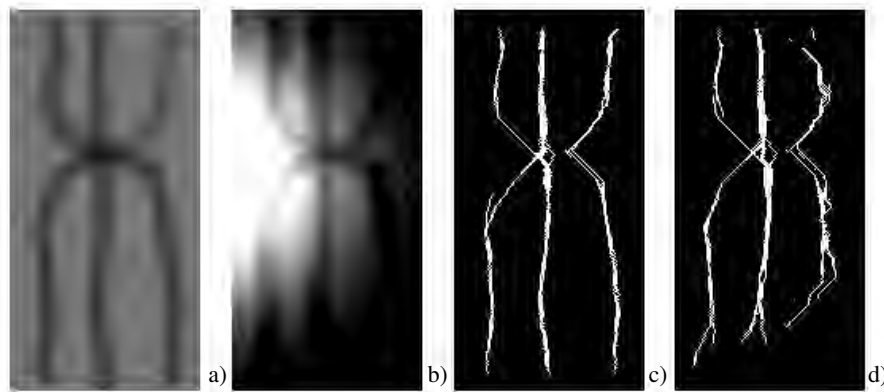


Fig. 11. Artificial vein image: a) original image, b) lightning conditions altered image, c) original image's product d) lightning conditions altered image's product

5 CONCLUSIONS

A overview of topics related to biometric systems with focus on vascular biometrics was discussed. A vein image preprocessing method which improves vein segmentation process was proposed. Feature extraction algorithm was described and implications of image displacement, rotation were analyzed, as well as impact of even versus uneven finger illumination. Tests were performed on both acquired vein and synthetic images. As mentioned in Light conditions subsection, proposed preprocessing method is suitable for evenly illuminated images. A more comprehensive method can be used, involving histogram equalization. Line tracking algorithm is a simple to implement algorithm, which can be easily customized in order to conform to the required application. It has, however, drawbacks, most important of which is bound to its random nature - the product of the algorithm is not repeatable. This results in *MPR* values approximately at 0.9 when matching products of the same input image. Another identified area of improvement is region of interest selection. Introducing this stage to both enrollment and matching flows would eliminate problems connected with finger displacement and rotation.

References

1. Jain, A. K., Ross A., Prabhakar S. (2004) An Introduction to Biometric Recognition, *IEEE Transactions On Circuit And Systems For Video Technology*, vol. 14, No. 1, 4-20.
2. Miura N., Nagasaka A., Miyatake T. (2004) Feature extraction of finger-vein patterns based on repeated line tracking and its application to personal identification, *Machine Vision and Applications 15*, Springer-Verlag, Berlin, Germany 194-203.
3. Chang S., Larin K. V., Mao Y., Flueraru C., Almuhtadi W. (2011) Fingerprint Spoof Detection Using Near Infrared Optical Analysis, *State of Art in Biometrics*, InTech, Rijeka, Croatia 57-84.
4. Wang K., Ma H., Popoola O. P., Li J. (2011) Finger Vein Recognition, *Biometrics*, InTech, Rijeka, Croatia 29-54.
5. Yang J., Shi Y. (2012) Finger vein ROI localization and vein ridge enhancement, *Pattern Recognition Letters* vol. 33, 1569-1579.
6. Yang L., Yang G, Yin Y., Xiao R. (2013) Sliding Window-Based Region of Interest Extraction for Finger Vein Images, *Sensors 13*, 3799-3815.
7. Horecker, B. L. (1943) The absorption spectra of hemoglobin and its derivatives in the visible and infra-red regions, *Journal of Biological Chemistry*, 148, Rockville, Maryland, 173-183.
8. Tower, J. R. et al. (2003) Large format backside illuminated CCD imager for space surveillance, *IEEE Transactions On Electron Devices*, vol. 50, issue 1, 218-224.
9. Song, W et al.. (2011) A finger-vein verification system using mean curvature *Pattern Recognition Letters*, vol. 32, 1541-1547.
10. Fronc, P (2012) Biometric systems - concept and data acquisition of finger vein patterns. In: Information Technology Theory and Application, A. Myśliński ed., IBS PAN, Warsaw, Poland, vol. 2, 23-35.

IDENTYFIKACJA NACZYŃ KRWIONOŚNYCH PALCA Z WYKORZYSTANIEM METODY ŚLEDZENIA LINII

Streszczenie. W niniejszej pracy opisano system weryfikacji biometrycznej operujący na wzorcach naczyń krwionośnych palca. Obraz pozyskiwany jest poprzez naświetlenie palca światłem podczerwonym, następnie poprzez filtr światła widzialnego, obraz trafia do kamery CCD. W celu poprawy jakości obrazu, został on poddany wygładzaniu. Wzorec naczyń został pozyskany za pomocą algorytmu śledzenia linii. W celu oceny działania algorytmu wykorzystano podejście statystyczne. Przedstawiono i omówiono wyniki eksperymentów numerycznych.

Słowa kluczowe: biometria naczyniowa, autentykacja biometryczna, pozyskiwanie obrazów

ISBN 83-894-7555-3